

Frequency-Dependent F-Number Increases the Contrast and the Spatial Resolution in Fast Pulse-Echo Ultrasound Imaging

Martin F. Schiffner and Georg Schmitz

Chair of Medical Engineering, Ruhr-University Bochum, 44801 Bochum, Germany

Copyright notice:

© 2021 IEEE. Personal use of this material is permitted. Permission from IEEE must be obtained for all other uses, in any current or future media, including reprinting/republishing this material for advertising or promotional purposes, creating new collective works, for resale or redistribution to servers or lists, or reuse of any copyrighted component of this work in other works.


Full citation:


2021 IEEE Int. Ultrasonics Symp. (IUS), Xi'an, China, Sep. 2021, pp. 1–4.

DOI: [10.1109/IUS52206.2021.9593488](https://doi.org/10.1109/IUS52206.2021.9593488)

[Click here for IEEE Xplore](#)

Frequency-Dependent F-Number Increases the Contrast and the Spatial Resolution in Fast Pulse-Echo Ultrasound Imaging

Martin F. Schiffner 
 Chair of Medical Engineering
 Ruhr-University Bochum
 Bochum, Germany
 martin.schiffner@rub.de

Georg Schmitz 
 Chair of Medical Engineering
 Ruhr-University Bochum
 Bochum, Germany
 georg.schmitz@rub.de

Abstract—Fixed F -numbers reduce grating lobe artifacts in fast pulse-echo ultrasound imaging. Such F -numbers result in dynamic receive subapertures whose widths vary with the focal position. These subapertures, however, ignore useful low-frequency components in the excluded radio frequency (RF) signals and, thus, reduce the lateral resolution. Here, we propose a frequency-dependent F -number to simultaneously suppress grating lobe artifacts and maintain the lateral resolution. This F -number, at high frequencies, reduces the receive subaperture to remove spatially undersampled components of the RF signals and suppress grating lobes. The F -number, at low frequencies, enlarges the receive subaperture to use the components of all RF signals and maintain the lateral resolution. Experiments validated the proposed F -number and demonstrated improvements in the contrast and the widths of wire targets of up to 3.2% and 12.8%, respectively.

Index Terms—dynamic aperture, F -number, fast ultrasound imaging, Fourier-domain beamforming, frequency-dependent apodization, grating lobes

I. INTRODUCTION

Software-based fast imaging modes combine high bandwidths with fully-sampled transducer arrays [1]–[3]. This combination, owing to large element pitch-to-wavelength ratios, suffers from spatial undersampling and requires a method to prevent image degradation. The formation of receive beams by small subapertures, which are defined by a fixed F -number and vary with the focal position (see, e.g., [4], [2, (3)]), avoids this undersampling and reduces grating lobe artifacts. These subapertures, however, ignore useful low-frequency components in the excluded radio frequency (RF) signals and, thus, reduce the lateral resolution. Here, we propose a frequency-dependent F -number to suppress image artifacts and approximately maintain the lateral resolution of the full aperture. We first derive a closed-form expression for this F -number from the far-field directivity pattern of a focused receive subaperture. We subsequently outline a simple Fourier-domain beamforming algorithm (see, e.g., [5], [6]) to implement this F -number and show its benefits in a phantom experiment.

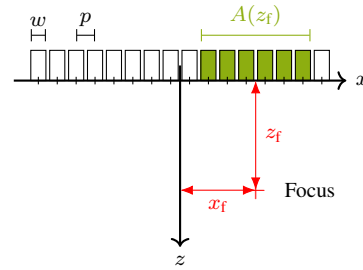


Fig. 1. Geometry of the uniform linear transducer array and definition of the F -number (1).

II. THEORY

The following derivations consider a uniform linear transducer array, as shown in Fig. 1, with N_{el} elements of width w and the element pitch $p \geq w$. A receive subaperture, which focuses a beam on the point (x_f, z_f) , consists of $N_{\text{sub}} \leq N_{\text{el}}$ elements and, unless indicated otherwise, is symmetric about the lateral focal coordinate x_f . The usual dispersion relation, i.e., $\lambda f = c$, links the product of the wavelength λ and the frequency f to the average speed of sound c .

A. What is the F -Number?

The F -number, for a uniform linear transducer array, equals the quotient of the focal length z_f and the width of the receive subaperture $A(z_f)$, i.e., [4], [2, (3)]

$$F = \frac{z_f}{A(z_f)}, \quad (1)$$

as shown in Fig. 1. The usage of a fixed F -number results in a dynamic receive subaperture whose width increases with the focal length. This increase, however, is limited by the finite aperture of the transducer array and, due to the discrete elements, discontinuous. The desired F -number, for these reasons, may differ from the actual F -number, especially for (i) large focal lengths or (ii) lateral focal coordinates x_f near the array bounds. Typical F -numbers range from 1 to 2 [7, p. 414].

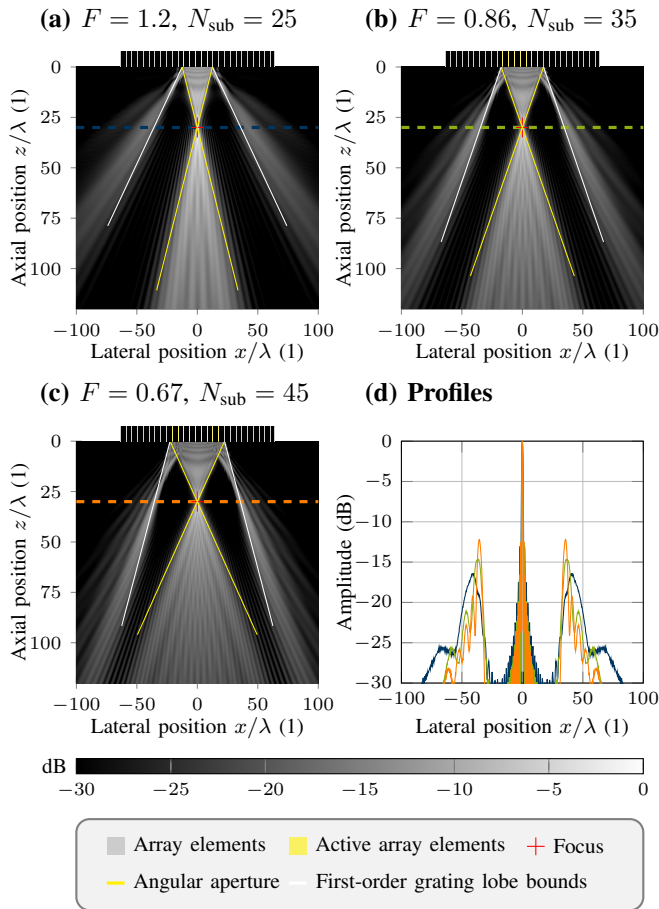


Fig. 2. Effect of the F -number (1) on a monofrequent receive beam. The focal length, the element width, and the element pitch amount to $z_f = 30\lambda$, $w = 0.981\lambda$, and $p = \lambda$, respectively. The receive subaperture is symmetric about the lateral focal coordinate $x_f = 0$.

B. Effect of the F -Number on the Image Quality

The F -number (1) trades off the lateral resolution against the suppression of grating lobe artifacts. This conclusion may be drawn from the effect of the F -number on a monofrequent receive beam, as shown in Fig. 2. The full width at half maximum (FWHM) of the main lobe in the focal plane decreases with the F -number (see also, e.g., [8, (8)]). Small F -numbers or, equivalently, large receive subapertures thus increase the lateral resolution. The first-order grating lobes, as the F -number decreases, however, move toward the main lobe and, owing to the directivity of the array elements, increase in amplitude. Large F -numbers or, equivalently, small receive subapertures thus reduce grating lobe artifacts.

C. Frequency Dependence of the Grating Lobe Angles

The frequency f , in addition to the F -number (1), strongly affects the position of the grating lobes. Since there is no simple closed-form expression for the receive beam in the focal plane, the far-field directivity pattern of the focused receive subaperture will be considered here. This pattern, for

each frequency, equals the Fourier transform of the aperture function and, omitting the derivation, reveals the identities

$$\sin(\alpha) = \frac{1}{\sqrt{1 + (2F)^2}} \quad \text{and} \quad \sin(\chi) = \frac{\lambda}{p} - \sin(\alpha), \quad (2)$$

where α denotes the angular half-width of the main lobe and χ is the angular distance of the first-order grating lobe. The movement of the first-order grating lobes toward the main lobe not only occurs for smaller F -numbers (1) but also for smaller wavelengths λ or, equivalently, higher frequencies f .

D. Proposed F -Number

An F -number that suppresses grating lobe artifacts up to an upper frequency bound and attempts to maintain the lateral resolution of the full aperture may be derived from the angular distance of the first-order grating lobe (2). The imposition of a minimum angular distance $\chi_{lb} \in (0, \pi/2]$ on this lobe yields the closed-form expression

$$F > F_{lb}(\chi_{lb}, \lambda) = \frac{1}{2} \sqrt{\frac{1}{\left[\frac{\lambda}{p} - \sin(\chi_{lb})\right]^2} - 1} \quad (3)$$

for $1/[1 + \sin(\chi_{lb})] < p/\lambda < 1/\sin(\chi_{lb})$. This expression is the smallest F -number that meets the grating lobe condition and, thus, maximizes the lateral resolution (see Subsect. II-B). Low frequencies, i.e., $p/\lambda \leq 1/[1 + \sin(\chi_{lb})]$, always permit the usage of the full aperture. High frequencies, i.e., $p/\lambda \geq 1/\sin(\chi_{lb})$, however, do not support the grating lobe condition and require separate measures. These measures are outside the scope of this paper. Larger F -numbers, which may result from the finite aperture, also meet the grating lobe condition but unnecessarily reduce the lateral resolution.

E. What Does the Proposed F -Number Accomplish?

The proposed F -number (3) not only eliminates grating lobe artifacts but also improves the lateral resolution. This F -number, at high frequencies, reduces the receive subaperture to remove spatially undersampled components of the RF signals and suppress grating lobes. The F -number, at low frequencies, enlarges the receive subaperture to use the components of all RF signals and maintain the lateral resolution of the full aperture.

III. IMPLEMENTATION

Our Fourier-domain beamforming algorithm [6] was enhanced to account for the frequency dependence of the proposed F -number (3). The resulting algorithm, first, decomposes the recorded RF signals into complex-valued Fourier coefficients by the fast Fourier transform. These coefficients, for each frequency and each image voxel, are then shifted in phase to compensate for the round-trip times-of-flight and weighted by a frequency-specific window function that reflects the width of the receive subaperture. The details of the implementation, e.g., the treatment of (i) the singularity of the proposed F -number (3) at $\lambda/p = \sin(\chi_{lb})$ and (ii) edge effects near the array bounds, are left to an additional publication. The

first author, however, maintains a public version of the Matlab¹ source code [5] to support the reproduction of the presented results and facilitate further research.

IV. EXPERIMENTAL VALIDATION

An experiment with a commercial multi-tissue phantom² (model: 040; average speed of sound: $c = 1538.75$ m/s) demonstrated the advantages of the position- and frequency-dependent receive subaperture selection by the proposed F -number (3). A SonixTouch Research system³ with a linear transducer array (model: L14-5/38; number of elements: $N_{el} = 128$, element width: $w = 279.8$ μm , pitch: $p = 304.8$ μm) acquired and stored the RF signals induced by eleven plane waves for offline processing. The excitation voltage was a single cycle at 4 MHz, and the steering angles ranged from -20° to 20° with a uniform spacing of 4° . The lower and upper bounds on the frequency f in the Fourier-domain beamforming algorithm (see Sect. III) were $f_{lb} = 2.25$ MHz and $f_{ub} = 6.75$ MHz, respectively, and resulted in element pitch-to-wavelength ratios p/λ between 0.45 and 1.34. The minimum angular distance of the first-order grating lobe in the proposed F -number (3) was set to $\chi_{lb} = 60^\circ$ and permitted the usage of the full aperture for element pitch-to-wavelength ratios p/λ up to 0.54. Both the full aperture and the smallest fixed F -number (1) that eliminated all visible grating lobe artifacts, i.e., $F = 1.5$, served as benchmarks. The generalized contrast-to-noise ratios (gCNRs) [9] of the anechoic regions and the axial and lateral FWHMs of all 16 wires measured the image quality.

V. RESULTS

The fixed F -number (1) eliminated all visible grating lobe artifacts but reduced the lateral resolution in comparison to the full aperture, as shown in Figs. 3(a) and 3(b) for a single plane wave. The proposed F -number (3) also eliminated these artifacts but increased the lateral resolution in comparison to the fixed F -number, as shown in Fig. 3(c). The median anechoic contrast, according to Fig. 3(d), amounted to 87.38 % for eleven steering angles and, thus, improved by 2 % and 3.2 % relative to the full aperture and the fixed F -number, respectively. The median FWHMs of the wires on the axial and lateral axes decreased by up to 2.9 % and 12.8 %, respectively, resulting in a volume reduction of up to 19.6 % for a single plane wave.

VI. CONCLUSION

The proposed combination of the frequency-dependent F -number (3) and the Fourier-domain beamforming algorithm (see Sect. III) improves the contrast and the lateral resolution, as summarized in Table I. Details of the implementation, such as the treatments of (i) the singularity of the proposed F -number (3) at $\lambda/p = \sin(\chi_{lb})$ and (ii) edge effects near

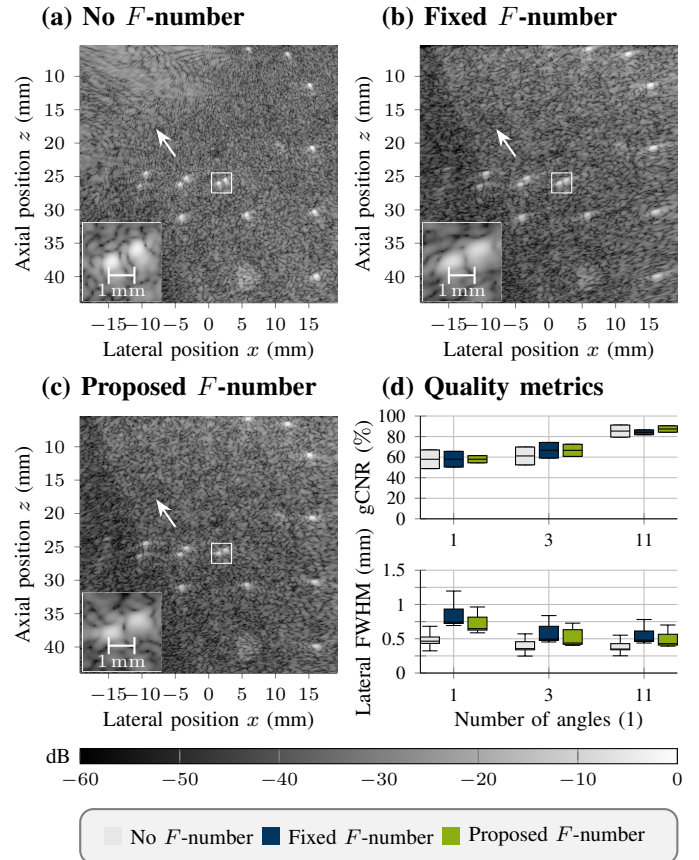


Fig. 3. Results for the multi-tissue phantom. The images show the absolute voxel values for the plane wave with the steering angle of -20° and (a) the full aperture, (b) the fixed F -number of $F = 1.5$, and (c) the proposed F -number (3) with $\chi_{lb} = 60^\circ$. The box plots (d) show the gCNRs of the anechoic regions (top) and the lateral FWHMs of the wires (bottom).

the array bounds, strongly influence the results and enable further improvements. The proposed combination is easier to implement and potentially faster than adaptive methods, such as minimum variance beamforming [10]. The frequency-dependent apodization weights, in fact, are independent of the RF signals and may be precomputed for a given geometry and bandwidth. Future research will investigate an efficient translation of the proposed combination into the time domain. Such a translation could base on filter banks and the usage of a piecewise constant F -number. This F -number would be fixed in each frequency band to enable standard time-domain receive beamforming. The F -number, however, would vary with the frequency band.

REFERENCES

- [1] M. Tanter and M. Fink, "Ultrafast imaging in biomedical ultrasound," *IEEE Trans. Ultrason., Ferroelectr., Freq. Control*, vol. 61, no. 1, pp. 102–119, Jan. 2014.
- [2] G. Montaldo, M. Tanter, J. Bercoff, N. Benech, and M. Fink, "Coherent plane-wave compounding for very high frame rate ultrasonography

¹The MathWorks, Inc., Natick, MA, USA

²Computerized Imaging Reference Systems (CIRS), Inc., Norfolk, VA, USA

³Analogic Corporation, Sonix Design Center, Richmond, BC, Canada

TABLE I. Properties of the Fixed F -Number (1) and the Proposed F -Number (3).

Method	Width of the receive aperture	Lateral resolution	Grating lobe suppression
No F -Number	Always full	Optimal	None
Fixed F -Number (1)	Focal position-dependent subaperture	Minimal	Exaggerated
Proposed F -Number (3)	Focal position- and frequency-dependent subaperture	Improved	Optimal

and transient elastography,” *IEEE Trans. Ultrason., Ferroelectr., Freq. Control*, vol. 56, no. 3, pp. 489–506, Mar. 2009.

- [3] J. A. Jensen, S. I. Nikolov, K. L. Gammelmark, and M. H. Pedersen, “Synthetic aperture ultrasound imaging,” *Ultrasonics*, vol. 44, Supplement, pp. e5–e15, Dec. 2006.
- [4] V. Perrot, M. Polichetti, F. Varray, and D. Garcia, “So you think you can DAS? A viewpoint on delay-and-sum beamforming,” *Ultrasonics*, vol. 111, p. 106309, Mar. 2021.
- [5] M. F. Schiffner, “Frequency-dependent F -number for coherent plane-wave compounding,” https://github.com/mschiffn/f_number, 2021.
- [6] M. F. Schiffner and G. Schmitz, “A low-rate parallel Fourier domain beamforming method for ultrafast pulse-echo imaging,” in *2016 IEEE Int. Ultrasonics Symp. (IUS)*, Tours, Sep. 2016, pp. 1–4.
- [7] T. L. Szabo, *Diagnostic Ultrasound Imaging: Inside Out*, 2nd ed. Elsevier Academic Press, Dec. 2013.
- [8] J.-Y. Lu, H. Zou, and J. F. Greenleaf, “Biomedical ultrasound beam forming,” *Ultrasound Med. Biol.*, vol. 20, no. 5, pp. 403–428, Jan. 1994.
- [9] A. Rodriguez-Molares, O. M. H. Rindal, J. D’hooge, S.-E. Måsøy, A. Austeng, M. A. Lediju Bell, and H. Torp, “The generalized contrast-to-noise ratio: A formal definition for lesion detectability,” *IEEE Trans. Ultrason., Ferroelectr., Freq. Control*, vol. 67, no. 4, pp. 745–759, Apr. 2020.
- [10] J.-F. Synnevåg, A. Austeng, and S. Holm, “Benefits of minimum-variance beamforming in medical ultrasound imaging,” *IEEE Trans. Ultrason., Ferroelectr., Freq. Control*, vol. 56, no. 9, pp. 1868–1879, Sep. 2009.